Effect of Ternary Addition on Characteristics of Pb-Sn Base Alloys

M.M. El-Sayed, F. Abd El-Salam, R.H. Nada, and M. Kamal*

Department of Physics, Faculty of Education, Ain Shams University, Cairo, Egypt.
**Metal Physics Lab, Physics Department, Mansoura University, Mansoura, Egypt.*

A study of the microaddition dependence of the structural, mechanical and electrical characteristics of lead-5wt.% Sn alloy prepared by melt spinning and/or the conventional method was carried out using X-ray diffraction, dynamic resonance technique, hardness and resistivity measurements. The conventional method produced more crystalline structure than that of the melt spun. The thermal diffusivity, hardness and resistivity values were found to be higher for PbSn samples prepared by the conventional method than those of the melt spun PbSn samples, while the value of the internal friction was higher for the melt-spun alloy samples. This may be due to the creation of defects by the rolling process used during the preparation of the cold rolled sheets. The dynamic Young's modulus was nearly of the same order for both the rapidly solidified and the cold rolled alloys. The results were explained in terms of the dislocation theory, the effect of quenching rate on the produced density fluctuations in composition and the modes of interaction of crystal lattice defects.

Introduction:

Lead base alloys, including binary and ternary alloys have been in common use since a very long time due to their easy and reliable castability, reasonable hardness and wear resistance, and their use as thin linings for heavy duity bearing. The solidification of alloys is complicated by solute partition at the interface between solid and liquid. The time necessary for the diffusion of atoms is the basis for the requirements that solidification takes place at an exceedingly slow rate. The high cooling rate in the melt-spinning technique makes the time necessary for diffusion insufficient to yield a solid alloy that is homogeneous in composition. In other words, solidification under nonequilibrium conditions will yield an alloy with composition far from uniform [1].

Heat transfer and fluid flow, in view of the various and complicated boundary conditions related to solidification process, affect the type of distribution and the scale of inhomogenities of the solid product. The concentration distribution of a solute in the solid is determined by solute transport in the liquid which depends on the thermal fluid flow through the environment near the interface. Solidification inhomogenities may be due to the segregation of the different elements forming the alloy during solidification of castings and ingots. The process of rapid solidification leads to the formation of amorphous and fine microstructures [2], new intermediate phases [3] and anomalous vacancy concentrations [4]. Deformation immediately after quenching facilitates the diffusion of excess quenched-in vacancies.

The deformation, at or near room temperature, increases the hardness and strength of nearly all metals. An alloy may be made sufficiently homogeneous for practical purposes if it is subjected to forging, rolling or any other working and then reheated to a temperature below its melting point. Small additions of impurity atoms alter profoundly the hardening kinetics of an alloy. The second phase in an alloy may be surrounded by the impurity atoms to reduce the lattice distortion, thus, diminish the available second phase atoms needed for zones or precipitates.

In Pb-Sn alloys directionally solidified in a positive thermal gradient, marcosegregation along the length of the sample takes place [5]. Pb-Sn eutectic alloy was reported to show outstandting super plasticity [6]. The addition of antimony to the solder Pb-Sn alloys gives the way to have a higher strength and lower plasticity compared to the lead-tin alloys. Some investigations show that addition of other elements such as silver or copper in certain industrial applications at certain level may be useful to produce alloys with desirable properties. It was suggested that alloying additions may interface with

nucleation event by changing the precipitate characteristics and/or boundary properties [7]. The nucleation and growth of the solid during solidification of Pb and Pb-Sn alloys were examined by electrical resistivity [8].

The present work aims to study the structure characteristics, mechanical and electrical properties of rapidly solidified ribbons and cold-rolled sheets of the Pb-Sn binary system, Fig. (1). Effect of addition of third element, namely Sb, Zn, Cu and Ag (0.5 wt. %), will be also considered.

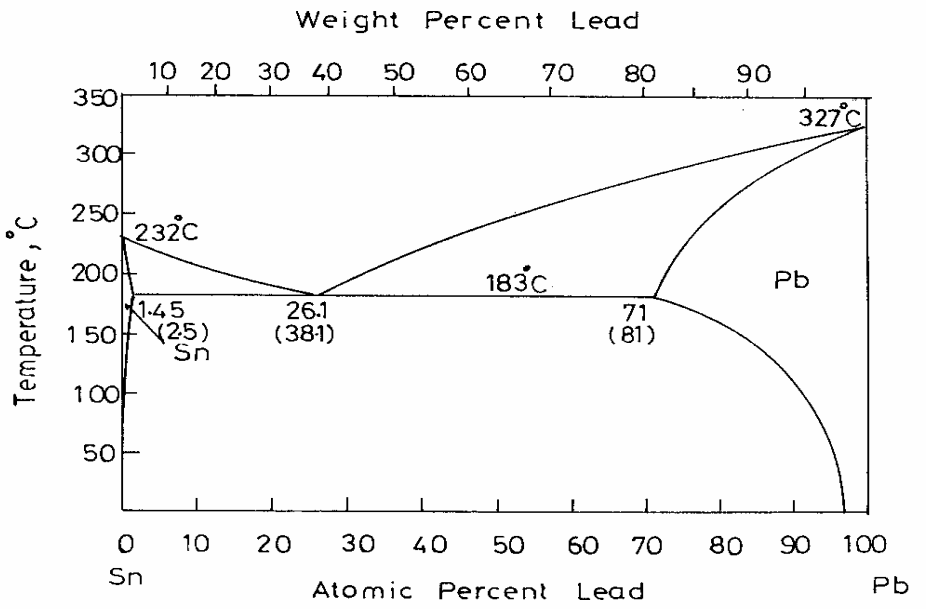

Fig. (1): The Pb-Sn equilibrium phase diagram.

Experimental:

A. Sample Preparation

In the present work, lead alloys were prepared from high purity elements (99.99%). To the base alloy lead-5wt.% Sn, 0.5wt.% of third elements, namely, Sb, Zn, Cu or Ag were added. The components were melted in an electric furnace at 1000 K. Some of the samples were prepared as ribbons by using the single roller type melt spinning technique, reported by Kamal et al. [1]. Melt spun ribbons were between 80 and 180 μm thick and 6 mm wide. The Solidification front velocity in the ribbons was estimated to be 30.4 m s^{-1}. The other prepared samples were cold rolled. The samples were obtained in the form of sheets 35 cm long, 7 mm width and about 200 μm thickness.

B. Measurements of Mechanical Properties:

The internal friction and the dynamic Young's modulus measurements were carried out with a modified dynamic resonance vibrator which vibrates electrodynamically [9]. The internal friction Q^{-1}, the dynamic Young's modulus Y and the thermal diffusivity D_{th} were obtained from the relations:

$$Q^{-1} = 0.5773 \frac{\Delta F}{F_0} \tag{1}$$

where F_o is the resonance frequency, ΔF is the full width at half maximum amplitude. The dynamic Young's modulus (Y) is given as:

$$Y = \left(\frac{2\pi L^2 F_0}{K Z^2} \right)^2 d \tag{2}$$

where d is the density of the sample under test, L is the length of the vibrating part of the sample, and K is the radius of gyration of the cross section about the axis perpendicular to the plane of vibration. The constant Z depends on the mode of vibration. For the fundamental mode, Z = 1.8751.

The thermal diffusivity D_{th} is given as:

$$D_{th} = \frac{2 t^2 F_0}{\pi} \tag{3}$$

where t is the thickness of the sample.

Hardness measurements were conducted on both the rapidly solidified and the cold rolled samples by using microhardness tester, Model FM.7 Future-Tech. Corp. Tokyo Japan. A load of 10 gm was applied for 5 s as indentation time, and the VHN was given automatically by the system.

C. Electrical Measurements:

Electrical resistivity measurements for the tested samples were made by using the Kelven Double-Bridge method in the temperature range from 290 to 440 K. The variation of temperature during the resistance - temperature investigation, was carried out by using a step-down transformer connected to a constructed temperature controller. The heating rate was kept constant during the investigation at 5 K min^{-1}.

D. X-ray diffraction measurements:

A Shimadzu X-ray diffractometer (DX-30) was used to trace t
he changes of structure through the analysis of the X-ray diffraction patterns obtained. The X-ray diffractometer has Cu-K_α radiation of wave length 1.542 Å working at 45KV and 35 mA. The scan speed was adjusted at 5 deg-min^{-1}. When the size of the individual crystals is less than about 10^{-5} cm, the term "crystallite size" is usually used. The crystallite size (t) can be calculated by the following equation, which is known as Scherrer formula [10].

$$t = \frac{0.9\lambda}{B\cos\theta} \qquad (4)$$

where B is the width of the diffraction line measured at half of the maximum intensity, λ is the wave length of the X-ray used and θ is the Bragg's angle at maximum intensity.

Results and Discussion:

a) The X-rays diffraction patterns obtained for the alloys; Pb-5wt.%Sn, Pb-5wt.%Sn-0.5wt.%Sb, Pb-5wt.%Sn-0.5wt.%Zn, Pb-5wt.%Sn-0.5 wt.%Cu and Pb-5wt.%Sn-0.5 wt.%Ag are illustrated respectively in Fig. 2 (a-e) for the melt-spun alloys and in Fig. 3(a-e) for cold rolled alloys, The patterns of all the melt-spun alloys revealed the presence of α-Pb (ICDD: 4-686) as well as a number of crystalline intermediate phases except of the Pb-5wt.%Sn which showed non-crystalline structure, Fig. (2a). The patterns in Fig. (2 b, d & e) contain sharp lines mainly due to α-Pb (ICDD: 4-686) in addition to some other phases such as β-Sn (ICDD: 4-673), SnSb, (ICDD: 1-830), CuSn (ICDD: 2-713) and AgSn (ICDD: 4-800). The formation and stability of amorphous alloys have been discussed with the concept of the alloying effect, configurational entropy, mixing enthalpy and chemical bonding [11]. The crystallite size of α-Pb phase was calculated from (111) plane for Pb- 5 wt.% Sn-0.5 Sb, Pb-5 wt.% Sn-0.5 Zn, Pb-5 wt.% Sn-0.5 Cu and Pb-5 wt.% Sn-0.5 Ag, are illustrated in Table (1) for both melt-spun and cold-rolled alloys. For Pb-5 wt.% Sn-0.5 Sb, melt-spun alloys pattern, the small crystallite size of the α-Pb phase as calculated from the (111) plane is 159 Å.

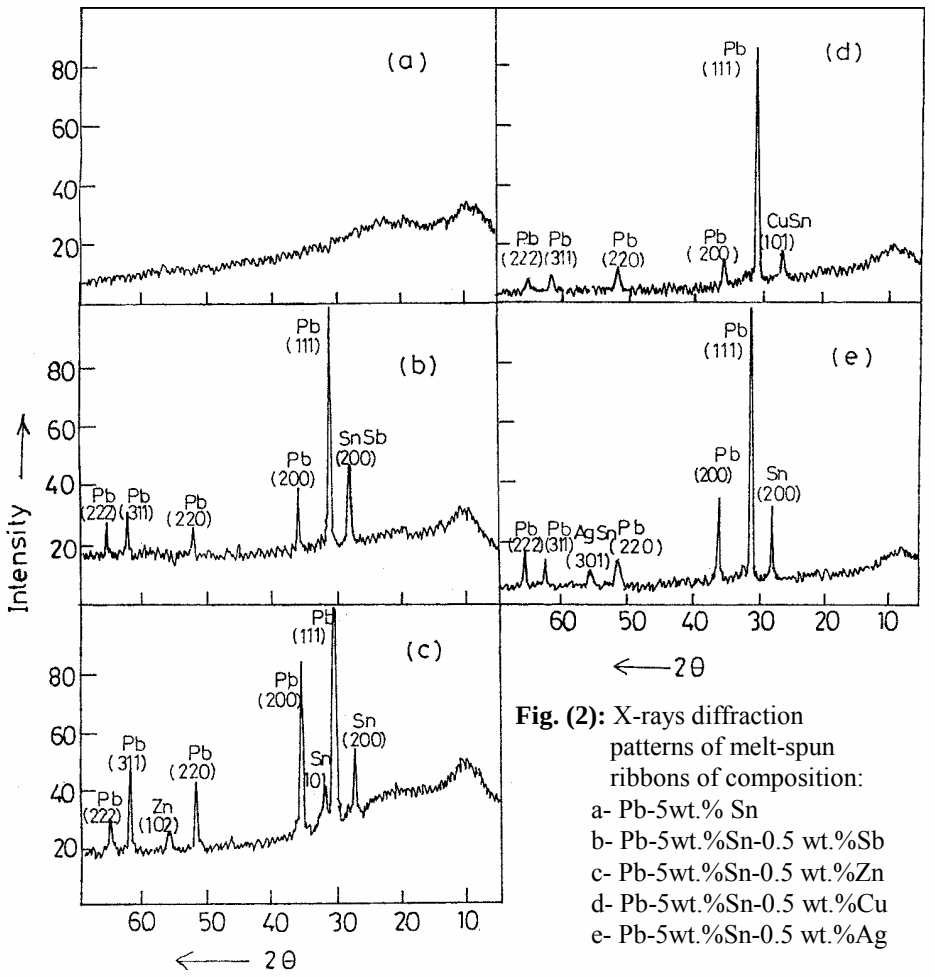

Fig. (2): X-rays diffraction patterns of melt-spun ribbons of composition:
a- Pb-5wt.% Sn
b- Pb-5wt.%Sn-0.5 wt.%Sb
c- Pb-5wt.%Sn-0.5 wt.%Zn
d- Pb-5wt.%Sn-0.5 wt.%Cu
e- Pb-5wt.%Sn-0.5 wt.%Ag

Table (1): Crystallite size in Å of α-Pb from (111) plane.

Composition	Melt-spun alloys	Cold rolled alloys
Pb-5wt%Sn-0.5wt%Sb	159	177
Pb-5wt%Sn-0.5wt%Zn	102	230
Pb-5wt%Sn-0.5wt%Cu	205	331
Pb-5wt%Sn-0.5wt%Ag	147	306

This might be due to the effect of solute atoms which lower the interfacial energy and consequently grain growth inhibition takes place leading to the small grain sizes obtained [12]. For Pb-5wt.% Sn-0.5 wt.% Zn melt-spun alloy pattern, α-Pb phase from the (111) plane has a crystallite size of 102Å. The crystallite size is small compared to the value obtained for Pb-5wt.%Sn-0.5

wt.%Sb. This might be rendered to the existing solute atoms (Zn). For Pb-5wt. % Sn-0.5 wt.%Cu, melt-spun alloy pattern contains sharp lines of the crystalline phase of α-Pb with crystallite size of 205 Å as obtained from the (111) plane. The crystallite size of α-Pb phase obtained from the (111) plane is 147 Å for Pb-5wt.%Sn-0.5 wt.%Ag, melt spun-alloy pattern.

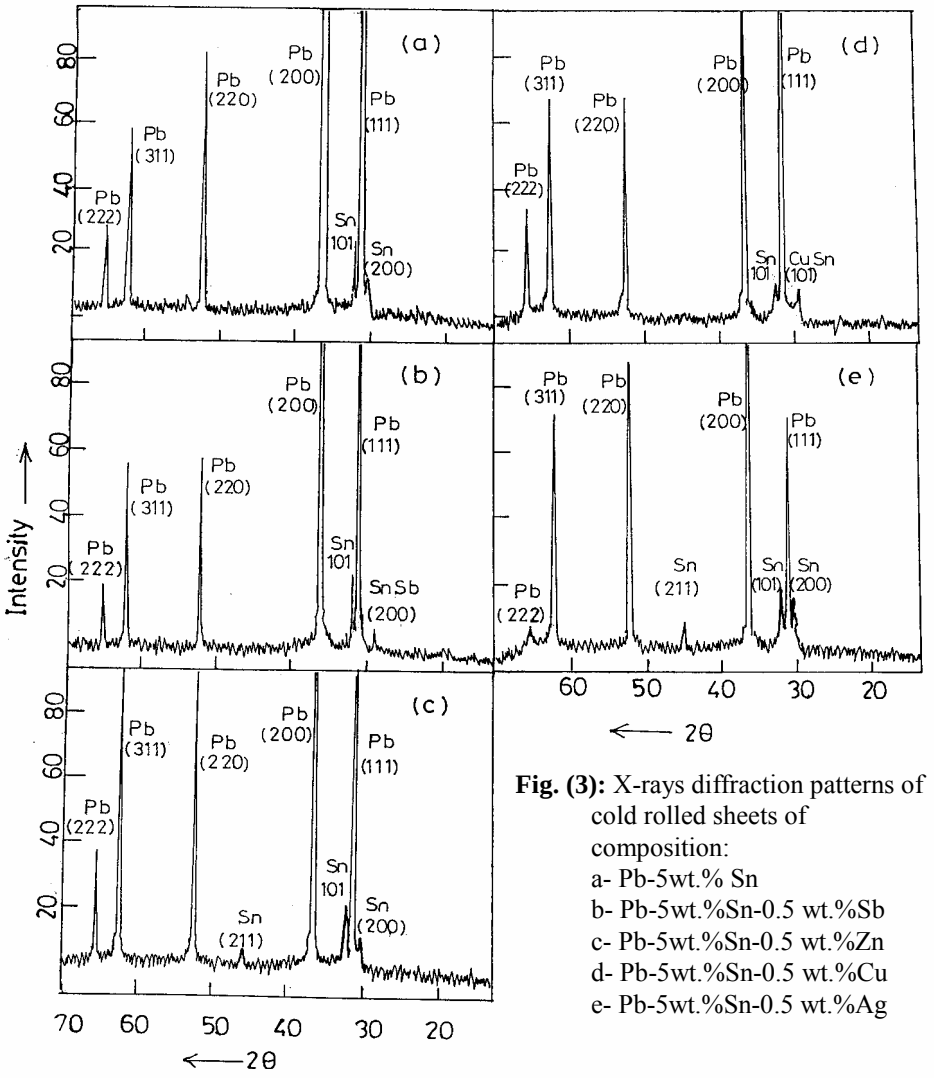

Fig. (3): X-rays diffraction patterns of cold rolled sheets of composition:
a- Pb-5wt.% Sn
b- Pb-5wt.%Sn-0.5 wt.%Sb
c- Pb-5wt.%Sn-0.5 wt.%Zn
d- Pb-5wt.%Sn-0.5 wt.%Cu
e- Pb-5wt.%Sn-0.5 wt.%Ag

The X-ray diffraction pattern for the cold-rolled Pb-5wt.%Sn-0.5 wt.%Sb, Pb-5wt.%Sn-0.5 wt.%Zn, Pb-5wt.%Sn-0.5 wt.%Cu, and Pb-5wt.% Sn-0.5 wt.%Ag, alloys Fig. (3). The crystallite sizes of the α-Pb phase for all these alloys as calculated from (111) planes are 177 Å, 230 Å, 331 Å and 306 Å, respectively

From the foregoing discussion it is clear that the cold rolled Pb-wt.%Sn based alloys are in general of crystalline nature than those rapidly solidified alloys. The crystallite sizes of the α-Pb phase of melt-spun alloys is smaller than that obtained from cold rolled alloys. This might be due to the relatively lower quenching rate of the cold rolled Pb-wt.%Sn based alloys compared with the corresponding melt-spun alloys.

b - The dynamic Young's modulus Y, internal friction Q-1, Vickers hardness Hv and thermal diffusivity Dth for Pb-5wt.%Sn, Pb-5wt.%Sn-0.5 wt.%Sb, Pb-5wt.%Sn-0.5 wt.%Zn, Pb-5wt.%Sn-0.5 wt.%Cu and Pb-5wt.%Sn-0.5 wt.%Ag alloys are illustrated in Table (2) for melt spun alloys and in Table (3) for cold rolld alloys, respectively. The maximum hardness of 6.5 Kg/mm2 for Pb-5wt. % Sn melt-spun alloy may be due to its noncrystalline structure. The melt-spun Pb-5wt. % Sn-0.5 wt.%Sb alloy has a maximum value for dynamic Young's modulus (26.22 GPa). This might be due to the existence of the SnSb as a hard inclusion causing difficult slipping of dislocations. The maximum values calculated for both the internal friction 16.7×10-2 and thermal diffusivity 11.24×10-9 cm2 s-1 for Pb-5wt.%Sn-0.5 wt.%Ag alloy might be due to the presence of the soft phases α-Pb and β-Sn.

Table (2): Mechanical and electrical properties of melt-spun alloys.

Composition	Dynamic Young's Modulus Y (GPa)	Hardness, VHN	Internal Friction ($Q^{-1}x10^{-2}$)	Thermal Diffusivity (D_{th} x 10^{-9}) (cm^2sec^{-1})	Resistivity at RT (Ωm x 10^{-7})
Pb-5wt.%Sn	20.05	6.5	11.8	9.1	3.2
Pb-5wt%Sn-0.5wt%Sb	26.22	6.2	10.1	6.5	1.4
Pb-5wt%Sn-0.5wt%Zn	16.8	5.6	10.8	6.5	4.0
Pb-5wt%Sn-0.5wt%Cu	24.5	4.15	9.9	4.13	2.04
Pb-5wt%Sn-0.5wt%Ag	14.05	5.12	16.7	11.24	5.54

Table (3): Mechanical and electrical properties of cold-rolled alloys.

Composition	Dynamic Young's Modulus Y (GPa)	Hardness, VHN	Internal Friction ($Q^{-1}x10^{-2}$)	Thermal Diffusivity (D_{th} x 10^{-9}) (cm^2sec^{-1})	Resistivity at RT (Ωm x 10^{-6})
Pb-5wt.%Sn	18.8	7.4	6.8	21	5.0
Pb-5wt%Sn-0.5wt%Sb	15.1	8.72	7.4	13.7	5.03
Pb-5wt%Sn-0.5wt%Zn	13.6	8.4	12.8	23	4.14
Pb-5wt%Sn-0.5wt%Cu	14.8	8.8	10.7	30.12	7.2
Pb-5wt%Sn-0.5wt%Ag	21.5	7.8	8.9	4.19	3.9

The lower values for hardness and internal friction belonging to the Pb-5wt.% Sn cold rolled alloy, might be due to the nature of crystalline defects of the cold rolled Pb-5wt.%Sn alloy. The maximum value for hardness and thermal diffusivity which belong to the Pb-5wt.% Sn-0.5 wt.%Cu cold rolled alloy might be due to the presence of the hard inclusion of $Cu_6 Sn_5$ compound.

Generally, the hardness and thermal diffusivity values are higher for the cold rolled alloys than those of the melt-spun alloys whose internal friction was higher. This might be due to the creation of defects by the rolling process during the preparation of cold rolled sheets [13], while dynamic Young's modulus was nearly of the same order for both the melt spun and cold rolled alloys.

The electrical resistivity measurements (ρ) for the Pb-5wt.%Sn based alloys, with the different microadditions, either rapidly solidified from the melt or cold rolled is shown in Fig. (4 a & b). It is clear that the resistivity of all alloys gradually increased up to a temperature of 440 K. A remarkable increase in the resistance values took place above 390 K for Pb-5wt.% Sn-0.5 wt.%Cu cold rolled alloy. This might be attributed to the nature of the existing compound CuSn. The small crystallite size of the compound, the large number of its dispersed particles and the less coherency of these particles with the matrix, which may exist, can probably cause anomalous increase in the resistivity at high temperature [12].

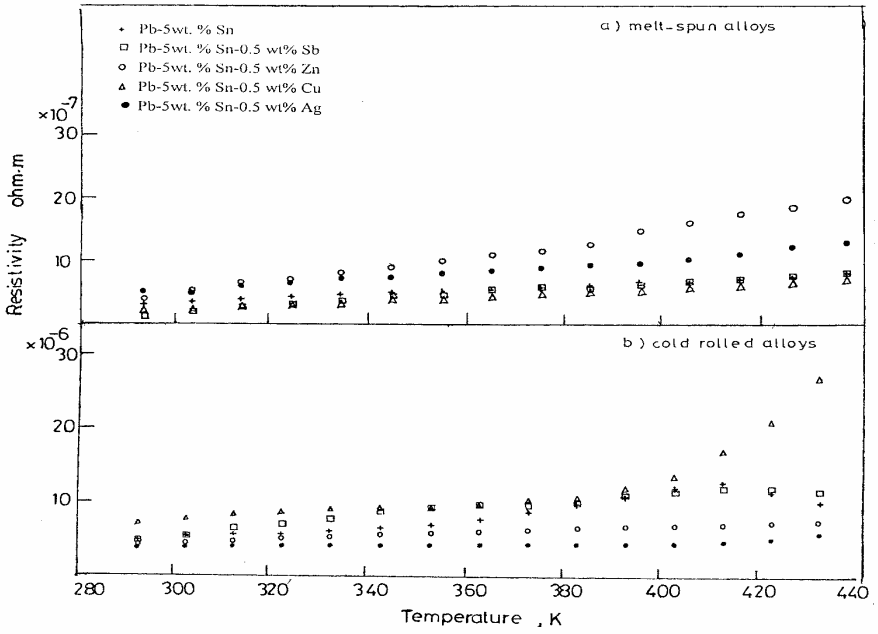

Fig. (4): Temperature dependence of electrical resistivity for Pb-5wt.%Sn with different microadditions.

The addition of Cu to Pb-5wt.%Sn melt-spun base alloy shows a decrease of the resistivity values than those of the other alloys in the tested range of temperature, Fig. (4 a). This might be attributed to the redistribution of solute Cu-atoms to form a homogenous solid solution Pb-5wt.%Sn-0.5 wt.%Cu melt-spun alloy. While the addition of Cu to Pb-5wt.%Sn cold rolled base alloys shows increased resistivity values, Fig. (4b). This increase of resistivity might be due to the increased solute atoms which act as scattering centers for the conduction charge carriers.

Generally, the resistivity values of the cold rolled alloys are higher than those of the melt-spun alloys. This may be due to the presence of defects created by the cold work introduced during the rolling process [13].

Conclusions:

The crystallite size of the different phases of melt-spun alloys is smaller than that obtained from cold rolled alloys. The cold rolled alloys are in general of crystalline nature than those rapidly solidified alloys. The hardness, thermal diffusivity and resistivity values are higher for the cold rolled alloys than those of melt-spun alloys.

References:

1. M. Kamal, J.C. Pieri and R. Jouty, Mém. Sci. Rev. Mét., Mars, 143 (1983).
2. N.R. Green, J.A. Charles, G.C. Smith, Mater. Sci. Technol. (UK) **10**, 11, 977 (1994).
3. Q.Li, E. Johnson, A. Johansen and L. Sarhoft-Kristensen, J. Mater. Res. **7**, 2756 (1992).
4. G. Thomas and R.H. Willens, Acta metall., **13**, 139 (1965), and **14**, 138 (1966).
5. S.N. Tewari, and R.Shah, Metall. Trans. A, Phys. Metall. Mater. Sci. (USA) **23 A** (12), 3383 (1992).
6. P.Zhang, Q.P.Kong and H.Zhou, Phil. Mag. A. Phys. Condens. Matter. Struct. Defects Mech. Prop. (UK) **77** (2), 437 (1998).
7. I.Manna and S.K. Pabi, phys. stat. sol. (a), **123**, 393 (1991).
8. S. H. Liu, D. R. Poilier and P. N. Ocansey, Metall. Mater. Trans. A, Phys. Metall. Mater. Sci., **26 A** (3), 741 (1995).
9. M. Kamal, A. M. Shaban, M. El-Kady and R. Shalaby, Radiation Effects and Defects in Solids, **138**, 307 (1996).
10. B. D. Cullity, "Elements of X-ray Diffraction", USA, 2nd Edn. (1959).
11. B. C. Glessen and C. N. J. Wagner in "Physics and chemistry of liquid Metals", Edt : S.Z. Bear, Marcel Dekker, New York, p. 633 (1972).
12. Structure and Propeoties of Malerials, Vol. IV, Electronic Properties, Robert M. Ras, lawrence A. Shepard, John Weilff, W.E.P. Ltd. 3rd Edn, p. 86-87, (1974).
13. V.B. John, " Introduction to Engineering Materials", 3rd Edn, p. 333 (1992).
14. M. Hansen, "Constitution of Binary Alloys", McGraw-Hill Publ. Co, New York, p. 1217 (1958).